Ministry of Higher Education and Scientific Research

Mohamed Boudiaf University of M'sila

FACULTY OF TECHNOLOGY
DEPARTMENT OF ELECTRONICS
N°: 2025/……..……

FIELD: SCIENCE AND TECHNOLOGY
BRANCH: ELECTRONICS
SPECIALIZATION : MICROELECTRONICS

Thesis Presented for the Achievement of the Academic Master's Degree

Presented by:

- Chemini Meriem

Title :

Ab-initio study of perovskite materials using CASTEP

Defended before the jury composed of:

…….	**University of Msila**	**President**
Pr. Idris bouchama	**Université M'sila**	**Supervisor**
Dr. Benlakhdar faiza	**Université M'sila**	**Co-Supervisor**
……	**University of Msila**	**Examiner**

Academic Year: 2024/2025

Dedicate

To the one who encouraged me to persevere throughout my life, to the man who has influenced my life the most, my dear father. To the one I rely on and depend on, to my kind-hearted beloved mother, and my dear sisters (Amal and Duaa) and brothers (Musa and Nour El Din), a special greeting to my fiancé (Tawfiq), my friend (Maryam), and to my friends, each by name. Whom I testify have supported and accompanied me.

Chemini meriem

Acknowledgement

*First and foremost, we would like to thank Almighty **ALLAH** for granting us the health and patience to complete this work.*

*We also want to express our deep gratitude to our supervisor **Professor BOUCHAMA Idris**, for initially proposing this topic and for his continuous follow-up throughout the preparation of this thesis, as well as for his ongoing advice and feedback.*

*We would also like to extend a special and heartfelt thank you to **Dr. Fayza Benlakhdar** for the tremendous efforts she has made for us. May Allah grant her health and well-being.*

*Additionally, we thank all the **Members of the Jury** for agreeing to review this work, as well as all our teachers from the Electronics Department.*

List of Figures

Chapter II: Physical properties of $BaTiO_3$

Chapter III: Results and discussions

List of Tables

Chapter II: Physical properties of $BaTiO_3$

Chapter III: Results and discussions

Table of contents

General Introduction

General introduction

Numerical simulation based on physical modeling has become increasingly widespread across diverse fields, from solid-state physics to molecular chemistry. Advances in computational power have enabled the use of sophisticated calculation techniques, improving the accuracy of experimental results. Among the theories that have revolutionized solid-state physics, Density Functional Theory (DFT) stands out. Developed by Hohenberg, Kohn, and Sham in the 1960s and 1970s, DFT describes the ground state of a system, and its practical application has become viable thanks to technological advancements. As a result, numerical simulation has emerged as a powerful tool for exploring various physical properties, reducing reliance on traditional experimentation. These computational methods offer faster, more cost-effective alternatives to physical trials while allowing researchers to manipulate material parameters and study their individual effects. Thus, digital simulations provide a means to preemptively analyze material behavior [1].

A thorough understanding of a material's structural, mechanical, and electronic properties—particularly its band structure—is essential for assessing potential applications. Optical properties, such as photon absorption, spontaneous and stimulated emission, as well as parameters like refractive index, dielectric function, and optical conductivity, play a crucial role in the development of advanced semiconductor components [2].

In this work, we focus on studying the structural, optical, and electronic properties of Barium Titanate ($BaTiO_3$) using CASTEP tool.

CASTEP is a widely used academic and commercial software package that employs density functional theory (DFT) with a plane-wave basis set to compute the electronic properties of crystalline solids, surfaces, molecules, and amorphous materials from first principles. It supports geometry optimization, molecular dynamics simulations, and the calculation of various derived electronic properties [3].

This dissertation is organized into three chapters:

Chapter one introduces the fundamental principles of Density Functional Theory (DFT), a cornerstone of quantum physics and chemistry. Unlike conventional methods that track individual electron movements, DFT describes a system’s energy in terms of electron density, providing a robust framework for predicting atomic and molecular behavior.

Chapter two explores the physical properties of $BaTiO_3$, covering its structural, electronic, and optical characteristics exist in bibliography.

Chapter three presents and analyzes the results obtained from CASTEP simulations, interpreting them in the context of the theoretical methods discussed earlier.

Finally, the conclusion summarizes the key findings and insights derived from this study.

References

[1] A. Djeffel, N. Hamidatou, Materials Physics Dissertation, "Study of the Structural, Electronic and Optical Properties of Ternary Alloys $BaSe_{1-x}S_x$," Larbi Ben M'hidi University, 2019.

[2] A. Khaldi, Doctoral Thesis in Science, University of Biskra, 2019.

[3] Payne, M. C., et al. (1992). Iterative Minimization Techniques for Ab Initio Total-Energy Calculations: Molecular Dynamics and Conjugate Gradients. Reviews of Modern Physics, 64(4), 1045-1097.

Chapter I

Density Functional Theory (DFT)

Chapter I: Density Functional Theory (DFT)

I.1 Introduction

Density Functional Theory (DFT) was initially proposed by Hohenberg and Kohn, with further development by Kohn and Sham by (Parr, Robert G, 1983) [1]. Despite initial skepticism, DFT has become a widely used computational method for predicting and analyzing electronic properties of materials [1].

In addition to DFT, several other ab initio codes are available for simulating and predicting material properties, including Quantum Espresso, Abinit, Castep, and VASP [2-5]. These codes have been extensively employed in studying various material types, such as metals, semiconductors and insulators.

DFT has been the primary tool for quantum mechanical simulation of periodic systems (P. Edwards *et al.*, 2013) [6]. Computational tools like DFT and other ab initio codes have played a crucial role in advancing material science research, enabling the design of materials with desired properties Robert R *et al.*, 1986) [7].

In conclusion, the development and applications of DFT and other ab initio codes have significantly contributed to material science research, leading to new discoveries and advancements in the field.

I.2 Schrödinger's equation

The Schrödinger equation is essential in the non-relativistic quantum description of crystalline or molecular systems. It serves as the foundation for this formalism and can be simplified through various approximations for ease of solution. To tackle the multi-body problem in quantum mechanics, the following Schrödinger equations [8,9] must be solved:

$$H\Psi = E\Psi \qquad \text{(I.1)}$$

Where E is the total energy of the system and Ψ is the wave function of the system.

H: Hamiltonian

The total Hamiltonian, denoted as H, is the Hamiltonian of the quantum system under study. In the non-relativistic case, it is written in the form:

Where:

TN: Kinetic energy of the nuclei:

$$H = T_N + T_e + V_{e-e} + V_{N-N} + V_{e-N} \quad \text{(I.2)}$$

$$T_N = \frac{-\hbar^2}{2M}\sum_k \Delta_k \quad \text{(I.3)}$$

T_e: Kinetic energy of the electrons:

$$T_e = \frac{-\hbar^2}{2m}\sum_i \Delta_i \quad \text{(I.4)}$$

$V_{e\text{-}e}$: Electron-electron interaction potential:

$$V_{e-e} = \frac{1}{2}\sum_{i,j\neq i} U_{ij} = \frac{1}{2}\sum_{i,j\neq i} \frac{e^2}{4\pi\varepsilon_0|\vec{r}_i-\vec{r}_j|} \quad \text{(I.5)}$$

$V_{N\text{-}N}$: Nuclei-nuclei interaction potential:

$$V_{N-N} = \frac{1}{2}\sum_{k,l\neq k} U_{kl} = \frac{1}{2}\sum_{k,l\neq k} \frac{e^2 Z_k Z_l}{4\pi\varepsilon_0|\vec{R}_k-\vec{R}_l|} \quad \text{(I.6)}$$

$V_{e\text{-}N}$: Electron-nuclei interaction potential:

$$V_{e-N} = \sum_{i,k} U_{ik} = \sum_{i,k} \frac{Z_k e^2}{4\pi\varepsilon_0|\vec{R}_k-\vec{r}_i|} \quad \text{(I.7)}$$

In an effort to simplify the notation, the spin coordinate was excluded. Nevertheless, the electrons' spin degree of freedom impacts the wave function.

I(r,t) and R(r,t), and therefore must be accounted. For stationary processes, the time-independent Schrödinger equation can be expressed as follows:

For electrons:

$$(-\hbar^2/2m)\nabla^2\Psi(r) + V(r)\Psi(r) = E\Psi(r) \quad \text{(I.8)}$$

For nuclei:

$$(-\hbar^2/2M)\nabla^2\Phi(R) + U(R)\Phi(R) = ER\Phi(R) \quad \text{(I.9)}$$

Where:

- ħ is the reduced Planck's constant;
- m is the mass of an electron;
- M is the mass of a nucleus;
- ∇^2 is the Laplacian operator.

Where V(r) represents the electron potential energy in terms of its spatial coordinates, U(R) represents the nuclear potential energy in terms of its spatial coordinates, E represents the total energy of the electron system and ER represents the total energy of the nuclear system.

Note: The equations provided assume a non-relativistic framework and neglect the spin-spin interactions between electrons and nuclei.

Where H is the Hamiltonian operator, Ψ is the wave function, E is the energy of the system, and the subscript "t" is omitted since the equation describes stationary states.

The total Hamiltonian operator (T H) for a system with multiple interacting particles, consisting of N nuclei and M electrons, can be obtained by adding the t. Total kinetic energy operator (T T) and the operator describing all Coulomb interactions (T V) in the Schrödinger equation.

The Hamiltonian operator plays a critical role in quantum mechanics as it describes the total energy of the system and is utilized to predict its time evolution.

The Schrödinger equation is essential in non-relativistic quantum mechanics for describing the behavior of crystalline or molecular systems. It encompasses the total energy of the system through the non-relativistic Hamiltonian operator, which includes the kinetic energy and Coulomb interactions. Solving the Schrödinger equation yields energy levels and wave functions that capture the system's dynamics.

The wave function must account for electron spin coordinates, introducing additional complexity. However, exact solutions are impractical for large systems due to the increasing number of particles. Consequently, simplifications are employed, such as the Born-Oppenheimer approximation, Density Functional Theory, and Hartree-Fock method (D. A. McQuarrie, 2007) [10].

The electromagnetic interaction becomes challenging for systems with numerous atoms and electrons, like solids with billions of nuclei and valence electrons. Without further simplification, solving the problem would be infeasible. Three common levels of simplification are the Born-Oppenheimer approximation, Density Functional Theory or Hartree-Fock approximation, and the approximations resulting from equation solving [11, 12].

I.2.1 Born Oppenheimer approximation

The Born-Oppenheimer approximation is a widely used technique in quantum mechanics to simplify the solution of the Schrödinger equation. This method assumes that the motion of the atomic nuclei is much slower than the motion of electrons, so the kinetic energy of the nuclei is neglected, and the Coulomb energy remains constant. Thus, the nuclei are considered to be stationary while the electrons move in their field. This approximation allows the separation of the electronic and nuclear motions, and the electronic Hamiltonian He is defined to describe the electronic behavior in the field of the nuclei. Using this Hamiltonian, the Schrödinger equation can be written to solve for the electronic wave function. The Born-Oppenheimer approximation is a fundamental concept in quantum chemistry and has many practical applications in molecular spectroscopy and electronic structure calculations [13,14].

Born-Oppenheimer approximation:

Schrödinger equation simplification:

$$\nabla^2\Psi(r,R) + (2\mu/\hbar^2)(E - V(R))\Psi(r,R) = 0 \qquad \text{(I.10)}$$

Electron motion decoupling from nuclear motion:

$$\Psi(r,R) = \psi(r)R(R) \qquad \text{(I.11)}$$

Nuclear kinetic energy term is neglected:

- T(R) ≈ 0
- Electron term:
- Electron wave function:
- ψ(r)
- Nuclear term:
- Nuclear wavefunction:
- R(R)

Electrostatic interaction between nuclei becomes constant:

$$V_{N-N} = constant \qquad \text{(I.12)}$$

Electron-nucleus interaction potential is approximated as an external potential independent of nuclear positions:

$$V_{e-N} = V_{ext} \quad \text{(I.13)}$$

Electronic Hamiltonian:

$$H_e = T_e + V_{ext} \quad \text{(I.14)}$$

Second level of approximation:

Hartree-Fock method (approximation on wave functions):

$$\nabla^2\psi_i(r) - 2\mu/\hbar^2\sum[V_{ext} + \sum(J(r) - K(r))]\psi_i(r) = \varepsilon_i\psi_i(r) \quad \text{(I.15)}$$

Density Functional Theory (approximation on Hamiltonian):

$$H_e[\rho(r)] = T_e[\rho(r)] + V_{ext} + \int \rho(r')v(r,r')dr' + Exc[\rho(r)] \quad \text{(I.16)}$$

The decoupling technique of separating electron and nucleus movements is an important approximation method in quantum mechanics for addressing N-body problems. This technique is discussed in academic works like "Introduction to Quantum Mechanics" by (D. J. Griffiths *et al.*, 2018) [15] and "Quantum Mechanics: Concepts and Applications" by (N. Zettili *et al.*, 2003) [16]. However, obtaining analytical solutions for the Schrödinger equation for electrons is challenging, except in simple cases like hydrogen. To overcome this challenge, various approximation techniques are utilized, as mentioned in the aforementioned sources.

I.2.2 Approximation of Hartree and Hartree.Fock

I.2.2.1 Hartree approximation

The Hartree-Fock approximation simplifies the behavior of multi-electron systems in quantum mechanics. It assumes that each electron moves independently in a mean field created by the other electrons and nuclei. By reducing the complex N-electron system to a single-electron system, the Hamiltonian can be expressed as the sum of the Hamiltonians for each electron. This approximation is widely studied and discussed in academic works such as "Introduction to Quantum Mechanics" by [15] and "Quantum Mechanics: Concepts and Applications" by [16]. The wave function of the entire electronic system is the product of the individual wave functions of each electron multiplied by their corresponding energies. The Hamiltonian for such a system is given by: [Hamiltonian equation].

$$H = \Sigma_{\mathrm{i=1}}^{\mathrm{N}} h(i) \quad \text{(I.17)}$$

Where h is the single-electron Hamiltonian.

$$\Psi(x_1; x_2; \ldots\ldots; x_N) = \varphi_i(x_1)\varphi_j(x_2)\ldots\ldots\ldots\ldots\varphi_k(x_N) \qquad \text{(I.18)}$$

represents the electronic wave function Ψ for a system of N electrons. The wave function is expressed as a product of single-electron wave functions φi, φj, ..., φk, where each wave function depends on the coordinates x1, x2, xN of the corresponding electron. This equation describes the spatial distribution of the electrons in the system, with each φ representing the probability amplitude of finding an electron at a specific position.

I.2.2.2 Hartree-Fock approximation

According to the article "Quantum Mechanics of Many-Electron Systems" by (P. A. M. Dirac, 1929) [17], the Hartree field can be used to break down a multiple equation into an equational system for a single electron. However, as [17] explain, the Hartree field neglects the exchange of any two particles, which means that the total wave function must be antisymmetric if the electron is a fermion. To address this, Fock suggested using Pauli's exclusion principle to correct the electron wave function, as mentioned in the article by [17], which can be expressed as a Slater determinant.

$$\Psi(r_1, r_2, \ldots, r\square) = 1/\sqrt{N!}\begin{vmatrix} \phi_1(r_1)\ \phi_2(r_1) & \phi\square(r1) \\ \phi_1(r_2)\ \phi_2(r_2) & \phi\square(r_2) \\ \cdot & \cdot \\ \cdot & \\ \phi_1(r\square)\ \phi_2(r_n) & \phi\square(r_n) \end{vmatrix}$$ (**Error! No text of specified style in document.**.1)

The results of this approximation are good, but they are only applicable to small molecules with few electrons.

I.3 Functional Density Theory (DFT)

The energy of an electronic system can be expressed in terms of the density of the ground state, denoted as ρ(r), which forms the basis of the density function. The theoretical model developed by Thomas and Fermi in 1920, which replaces the calculation of the wave function dependent on 3N spatial coordinates with a simpler function, the electron density that depends only on 3 spatial coordinates, is the origin of the DFT (Functional Density Theory). Hohenberg and Kohn, as well as Kohn and Sham, made significant contributions to the field in the 1960s. The Thomas-Fermi model is a remarkable concept in the field of quantum mechanics, as it simplifies the complex calculation of the electron density. The

details on this model are available in the works of Thomas and Fermi (1927), (Hohenberg and Kohn, 1964) [18], and (Kohn and Sham, 1965) [19].

Let us recall that the electron density, ρ(r), in an electronic system represents the number of electrons per unit volume in a given state (or the probability of finding an electron in a unit volume). It can be defined as:

$$\rho(r) = |\Psi(x_1, x_2, \ldots, x_N)|^2 \quad \text{(I.20)}$$

Here, Ψ represents the wavefunction of the system, and N represents the total number of electrons. The electron density ρ(r) approaches zero as r tends to infinity, and when integrated over all space, it equals the total number of electrons N:

$$\int \rho(r) dr = N \quad \text{(I.21)}$$

In 1964, Hohenberg and Kohn introduced two theorems to establish a mathematical framework for earlier concepts. These two theorems form the basis of the current form of DFT (Density Functional Theory).

I.3.1 Thomas-Fermi model

The work of Hohenberg and Kohn (1964) [18] initiated the development of density functional theory in 1964 and 1965. Their publications introduced two theorems that are considered the cornerstone of DFT.

- **First theorem:**

The relationship between the total energy E of an electronic system's ground state and its density ρ(r) under a specific external potential Ve(r) was established through a theorem [18]. According to this theorem, knowing the electron density enables the determination of all wave functions. Consequently, a ground-state electron density functional denoted by E[ρ(r)] is utilized to represent the total energy E of an electronic system interacting in an external potential [18].

- **Second theory:**

Every multiparticle system has a total functional energy, the minimum corresponding to the ground state. Ground-state particle density confirms:

According to the work of Hohenberg and Kohn (1964) [18], the actual density of the ground state is the one that minimizes the energy E. In fact, all other properties of the system are also dependent on this density. Vibration analysis is a method that is commonly

employed to calculate the ground state energy of an electronic system when it is subjected to an external potential.

I.3.2 Hohenberg.Kohn theorems

The fundamental formalism of Density Functional Theory (DFT) applies to systems with multiple interacting particles that evolve in an external potential, and is rooted in the Hohenberg-Kohn theorem (Hohenberg & Kohn, 1964) [18]. The Hohenberg-Kohn theorem is based on two underlying theorems that provide a framework for DFT, making it a widely applicable tool for studying electronic structure and properties of materials (Kohn & Sham 1965) [19].

- **Theorem I:**

According to this theorem, the electron density function (r) is sufficient to determine all electronic properties of a system. This means that the ground state electron density 0(r) and the external potential Vext(r) have a direct correspondence, and similarly, the wave function of the ground state background(r) and background(r) also correspond. The energy functional E [ρ, Vext] can be written as an integral consisting of two parts. The first part is the integral of the external potential Vext multiplied by the electron density ρ(r):

$$E[\rho, V_{ext}] = \int V_{ext}\rho(r)dr + FHK[\rho] \quad \text{(I.22)}$$

In this equation, FHK[ρ] represents the universal HK functional that combines the universal terms of electron kinetic energy T(ρ) and the potential energy due to electron-electron interaction Ve-e. It can be written as:

$$FHK[\rho] = T[\rho] + V_e - e[\rho] \quad \text{(I.23)}$$

The second theorem of Hohenberg and Kohn attempts to answer the question of how to determine whether any density is that of the ground state, given that it is known that the electronic density of the ground state is sufficient to obtain all the properties of this state.

- **Theorem II:**

This theorem demonstrates that the energy functional E is minimal when any electron density corresponds to the electron density of the ground state background(r).

In this theorem, the energy functional E[ρ(r)] that provides access to the ground state energy is minimized when the electron density exactly matches that of the ground state.

$$E = minE[\rho(r)] \quad \text{(I.24)}$$

In other words, according to the first theorem, a test wave function and a test Hamiltonian are both defined for a test electron density. From this, we can establish a correspondence between the wave function of the variational principle and the electronic density versions.

However, an important problem remains to be solved: how to rewrite an exact analytical formulation of the FHK functional for an interacting N-electron system?

I.4 Kohn and Sham equations

The description of kinetic energy and electron-electron interactions in terms of electron density is a challenging mathematical problem when considering a system of interacting electrons in motion. In an attempt to solve this problem, Kohn and Sham introduced a theoretical approach, known as the Kohn-Sham equations (Kohn and Sham, 1965) [19]. This approach replaces the actual electronic system with a hypothetical system, in which each electron behaves independently and is only influenced by an effective potential, the Kohn-Sham potential. The potential comprises both the external potential caused by the nuclei and the potential induced by the influence of other electrons on the electron of interest.

K-S (Kohn-Sham) reformulated the energy functional of the real system based on the fictitious system. The reformulated energy functional is expressed as:

$$E[\rho(r)] = T_0[\rho(r)] + V_{ee}[\rho(r)] + V_{ex}[\rho(r)] + Exc[\rho(r)] \quad \text{(I.25)}$$

In this expression, $T_0[\rho(r)]$ represents the kinetic energy of non-interacting particles, $V_e[\rho(r)]$ represents the classical Coulomb contribution known as the Hartree energy, and $Exc[\rho(r)]$ is the exchange-correlation functional.

The total energy (E) is given by:

$$E = [T[\rho] - T_0[\rho]] + V[\rho] + V_{ee}[\rho] + V_{ex}[\rho] \quad \text{(I.26)}$$

Where $V[\rho]$ is the external potential term and $[\rho]$ is the density-density interaction term.

The exchange-correlation potential (V_{ext}) is calculated from the derivative of the exchange-correlation energy functional (Exc) with respect to the electron density ($\rho(r)$):

$$V_{ex} = \partial EX[\rho(r)]/\partial\rho(r) \quad \text{(I.27)}$$

$(HKS(r) - \varepsilon_i)\phi_i(r) = 0$ (**Error! No text of specified style in document.**.2)

By introducing the Kohn-Sham framework, the Schrödinger equation is transformed into N single-electron Schrödinger equations, commonly known as the Kohn-Sham equations:

Here, HKS is the Kohn-Sham Hamiltonian, N represents the number of electrons, and ε_i are the eigenvalues. The Kohn-Sham Hamiltonian is defined as:

$$HKS = -\nabla^2 + V_eff(r) \quad \text{(I.29)}$$

The effective potential (V_eff(r)) is given by:

$$V_eff(r) = V_classical[\rho(r)] + V_{ee}[\rho(r)] + V_xt[\rho(r)] + V_{ex}[\rho(r)] \quad \text{(I.30)}$$

The electron density (ρ(r)) is determined from the N single-electron wave functions $\phi_i(r)$:

$$\rho[r] = \sum \phi_i(r)^2 \quad \text{(I.31)}$$

Where the sum runs from i = 1 to N.

I.4.1 Exchange and correlation energy approximations

I.4.1.1 Local density approximation (LDA)

The exchange-correlation energy of an inhomogeneous electron system can be determined using a method based on the assumption that the electron density is constant in each infinitesimal volume that makes up the actual system (J. P. Perdew, 1981) [20]. The exchange energy of the density of each volume is then estimated using the exchange energy obtained from a uniform electron gas (J. P. Perdew *et al.*, 2008) [21]. This estimated exchange energy is considered as the exchange energy of the corresponding density. The total energy of exchange-correlation of the system can be expressed as the sum of the exchange energies of all the infinitesimal volumes of the system. The equation is:

$$Exc = \int \rho(r)\varepsilon xc[\rho(r)]dr \quad \text{(I.32)}$$

In this equation, εxc[ρ(r)] represents the exchange-correlation energy density for a homogeneous electron gas. It can be decomposed into the exchange energy density (εx[ρ(r)]) and the correlation energy density (εc[ρ(r)]):

$$\varepsilon xc[\rho(r)] = \varepsilon x[\rho(r)] + \varepsilon c[\rho(r)] \quad \text{(I.33)}$$

The exchange energy density (εx[ρ(r)]) and the correlation energy density (εc[ρ(r)]) correspond to the exchange and correlation contributions of a homogeneous electron gas, respectively. The Dirac exchange function precisely identifies the analytical expression of exchange energy:

$$\varepsilon x(r) = Cx\rho^3 \quad \text{(I.34)}$$

Where:

$$Cx = -(3/4\pi)^(1/3) \quad \text{(I.35)}$$

The exchange energy density (εx[ρ(r)]) and the correlation energy density (εc[ρ(r)]) correspond to the exchange and correlation contributions of a homogeneous electron gas, respectively. The Dirac exchange function precisely identifies the analytical expression of exchange energy:

I.4.1.2 Generalized Gradient Approximation (GGA)

According to a scientific article by (J. P. Perdew *et al.,* 1996) [22], the Local Density Approximation (LDA) considers the density at a given point r, but in real systems, the density is not homogeneous throughout space, which makes it more practical to include a correction that considers the rate of change of r. To address this issue, the Generalized Gradient Approximation (GGA) introduces a correction to the exchange-correlation energy functional that takes into account the local charge concentrations and their gradients. The GGA functional is defined in a general form that allows for a more accurate calculation of electronic properties in real systems with spatially inhomogeneous densities.

The exchange-correlation functional is expressed in terms of the electron density (ρ) and its gradient (∇ρ) according to the following equation:

$$E_{GGA}[\rho] = \int \rho(r)\varepsilon_{GGA}[\rho(r), \nabla\rho(r)]d^3r \quad \text{(I.36)}$$

In this equation, ƐGGA[ρ(r), ∇ρ(r)] represents the generalized exchange-correlation energy (GGA) depending on both the electron density and its gradient.

Often, the contributions for exchange (εx) and correlation (εc) are separately developed in the GGA functional.

$$GGA[\rho, \nabla\rho] = GGA[\rho, \nabla\rho]x + GGA[\rho, \nabla\rho]c \quad \text{(I.37)}$$

Where GGA[ρ,∇ρ]x corresponds to the exchange contribution, and GGA[ρ,∇ρ]c corresponds to the correlation contribution. The GGA functional can also include other terms

and coefficients denoted as Zxc. Additionally, the electron density (∇ρ) can represent the gradient of the electron density with respect to spatial coordinates.

According to a research paper by (B. Hammer *et al.*, 1999) [23], there exist various forms of exchange-correlation (Exc) functionals in density functional theory. Among these, the functionals developed by Perdew and Wang (PW91), Perdew and Becke (B88), and Burke and Ernzerhof have gained popularity due to their accuracy and ease of implementation. These functionals are commonly used for electronic structure calculations in different fields of science and engineering.

I.5 Solving the Kohn-Sham equation

The Kohn-Sham equation is a fundamental equation in density functional theory (DFT) that describes the behavior of non-interacting electrons in an effective potential. The equation can be written as:

$$[-1/2\nabla^2 + v_eff(r)]\psi_i(r) = \varepsilon_i\psi_i(r) \quad \text{(I.38)}$$

Where ψ_i(r) is the wave function of the i-th electron, ε_i is its energy, and v_eff(r) is the effective potential, which is a sum of the external potential and the Hartree and exchange-correlation potentials. The Hartree potential is given by:

$$v_H(r) = \int \rho(r')/|r - r'|dr' \quad \text{(I.39)}$$

Where ρ(r) is the electron density. The exchange-correlation potential is a functional of the electron density and is typically approximated using density functionals such as the local density approximation (LDA) or the generalized gradient approximation (GGA).

The process of solving the Kohn-Sham equation involves finding the eigenvalues and Eigen functions through numerical methods such as the self-consistent field (SCF) method or direct minimization. The SCF method iteratively solves the Kohn-Sham equation until self-consistency is achieved, meaning that the electron density matches the density used to calculate the effective potential. Detailed information on the Kohn-Sham equation and its solutions in density functional theory (DFT) calculations can be found in various research papers and textbooks. Some relevant references include "Density Functional Theory: A

Practical Introduction" by (J. A. Steckel *et al.*, 2009) [24], as well as the research papers by Kohn and Sham (1965) [19] and Hohenberg and Kohn (1964) [18].

I.6 Pseudo-potential methods and plane waves

I.6.1 Introduction

Pseudo potential methods and plane wave basis sets are widely used in solid-state physics and materials science to study the electronic structure of materials. Pseudo potential methods are a class of approximations used to simplify the calculation of electronic structure in solids, while plane wave basis sets are used to represent the wave functions of electrons in a crystalline solid.

Pseudo potential methods were first introduced in the 1950s and have since become a powerful tool for studying electronic structure in materials. The basic idea of pseudo potential methods is to replace the complicated atomic potentials that describe the interaction between electrons and atomic nuclei with a simplified potential that only includes the core electrons. This simplification reduces the computational cost of electronic structure calculations and allows for the study of larger and more complex systems. One of the earliest works in this field was by Hohenberg and Kohn in 1964 [18], where they presented their density functional theory (DFT) and its application to solids.

Plane wave basis sets, on the other hand, are a type of basis set used to represent the wave functions of electrons in a crystalline solid. The wave functions are expanded in terms of plane waves, which have a well-defined momentum and wavelength, and are periodic in space. The use of plane wave basis sets allows for the accurate description of electronic structure in materials, particularly in the case of metals and semiconductors.

One of the earliest works on this topic was by (F. Bloch 1929) [25], who developed the concept of Bloch waves to describe the wave functions of electrons in a crystalline solid.

The combination of pseudo potential methods and plane wave basis sets has proven to be a powerful tool for the study of electronic structure in materials. This approach is commonly used in software packages such as Quantum ESPRESSO and VASP to simulate and analyze materials at the atomic scale. The accuracy of these methods has been continuously improved over the years, and they are now widely used in the field of materials science.

In conclusion, the combination of pseudo potential methods and plane wave basis sets has become a powerful tool for the study of electronic structure in materials. The development of these methods was influenced by early works of Hohenberg and Kohn, and Bloch. These methods are now widely used in software packages such as Quantum ESPRESSO and VASP to simulate and analyze materials at the atomic scale.

I.6.2 Bloch Theorem (the plane wave approach)

The Bloch theorem, first introduced by Felix (F. Bloch, 1928) [26], is a fundamental principle in the study of periodic structures. It relates the electronic wave function in a crystalline solid to its periodic potential. According to the Bloch theorem, the wave function of an electron in a periodic potential can be written as a product of a plane wave and a periodic function, which is known as the Bloch function. The plane wave represents the free electron propagation, while the periodic function describes the periodicity of the crystal lattice. The Bloch theorem is expressed mathematically as:

$$\Psi(r + R) = e^{(ik \cdot R)}\psi(r) \qquad \text{(I.40)}$$

Where ψ (r + R) is the wave function at a point shifted by a lattice vector R, e(ik·R) is a phase factor, k is the wave vector, and ψ(r) is the wave function at the original point. This equation shows that the wave function of an electron in a crystal has the same form at any two points that differ by a lattice vector R. The wave function is periodic with respect to the lattice, and its periodicity is characterized by the wave vector k.

The Bloch theorem has important implications for the electronic structure of solids. It explains why the energy bands in a crystal are formed, and why they have the periodicity of the lattice. The electronic states in a crystal are labeled by their wave vectors, which are restricted to a Brillouin zone, the first Brillouin zone being the primitive cell of the reciprocal lattice. The band structure of a crystal can be calculated by solving the Schrödinger equation for the Bloch functions. The Bloch theorem has been used extensively in the study of semiconductors, metals, and insulators, and is the basis for many important concepts in solid-state physics, such as the Fermi surface, the density of states, and the effective mass approximation.

I.6.3 Sampling of the first Brillouin zone

The Brillouin zone (BZ) is a periodic region in reciprocal space that encompasses wave vectors k with the same periodicity as the crystal lattice. The first Brillouin zone (FBZ) is

the smallest region enclosing the origin and a single unit cell of the lattice. Sampling the FBZ is crucial in electronic band Monk Horst-Pack method utilize a uniform grid of k-points (H. J. Monkhorst *et al.*, 1976) [27], while the Matthiessen-Paxton method employs a smearing function for broadening the k-point grid (M. Methfessel *et al.*, 1989) [28].

The choice of sampling scheme and the number of k-points significantly affects accuracy and efficiency. More complex band structures or precise calculations of properties like density of states or optical properties require denser k-point sampling (G. Kresse *et al.*, 1996) [29].

In summary, accurate electronic band structure calculations necessitate sampling the FBZ, where the choice of sampling scheme and number of k-points impacts accuracy and efficiency. Equation:

The k-point mesh is defined as follows:

$$\Gamma = (1/N_{1,1}/N_{2,1}/N_3) \quad \text{(I.41)}$$

Where N1, N2, and N3 are the number of k-points along each reciprocal lattice vector in the Brillouin zone [27].

The total number of k-points required to sample the Brillouin zone is given by:

$$N = N_1 x N_2 x N_3 \quad \text{(I.42)}$$

Where N is the total number of k-points [27].

Another important concept is the weight of each k-point, which is determined by the size of the Brillouin zone and the number of k-points used for sampling. The weight of a k-point is given by:

$$W_k = (1/VBZ)x(2\pi)^3/N \quad \text{(I.43)}$$

Where VBZ is the volume of the Brillouin zone.

I.6.4 Ecut-off energy

The cut-off energy (Ecut) is a crucial parameter in density functional theory (DFT) calculations of electronic band structures and related properties. It determines the size of the basis set used to expand the electronic wave functions as plane waves.

Choosing a sufficiently high Ecut is vital for accurate results in properties like total energy, density of states, and optical properties. However, excessively high Ecut values increase computational costs, while insufficient values introduce significant errors.

Methods such as convergence testing involve calculating properties for increasing Ecut values until convergence to a stable value is achieved (S. Baroni *et al.*, 2001) [30].

Another approach is the extrapolation method, where properties are extrapolated to the limit of infinite Ecut (D. Vanderbilt, 1990) [31].

The appropriate value of Ecut depends on the system's size, complexity, and desired accuracy, with larger systems and higher accuracy requirements generally necessitating higher Ecut values [5].

In summary, selecting an appropriate value of Ecut is crucial for accurate and efficient DFT calculations of electronic band structures and related properties.

The plane wave basis set is defined as follows:

$$\Psi(r) = \sum GC(G)exp(iG \cdot r) \quad \text{(I.44)}$$

Where Ψ(r) is the electronic wave function at position r, G is a reciprocal lattice vector, C(G) is the expansion coefficient for wave vector G, and the sum is over all reciprocal lattice vectors G within a sphere of radius Ecut centered on the origin of the reciprocal space [5].

I.7 CASTEP Simulation tool

CASTEP (Computer Aided Simulation of Thermochemistry and Energy of Materials) is a powerful computational tool for the simulation of materials at the atomic level. It is a widely used code for first-principles electronic structure calculations based on density functional theory (DFT). CASTEP can simulate a variety of properties of materials, such as crystal structures, electronic structures, optical and magnetic properties, and chemical reactions.

CASTEP uses a plane-wave basis set to expand the electronic wave functions and a pseudo potential approximation to describe the ion-electron interaction. The code can handle both periodic and non-periodic boundary conditions, making it suitable for the simulation of surfaces, interfaces, and nanoparticles.

One of the key features of CASTEP is its ability to perform calculations at different levels of theory, such as the local density approximation (LDA), generalized gradient

approximation (GGA) and hybrid functional. The code also includes several advanced features, such as the calculation of phonon dispersions and the simulation of solid-state NMR and EPR spectra.

CASTEP is user-friendly and can be run through a graphical user interface or via command-line interface. The code is maintained and updated regularly, and it has an active user community that provides support and shares expertise.

In summary, CASTEP is a powerful tool for the simulation of materials at the atomic level. It is widely used in academia and industry and provides a broad range of simulation capabilities for the study of various properties of materials.

I.8 Conclusion

In conclusion, density functional theory (DFT) has become an essential tool for studying the electronic structure and properties of materials. DFT provides a rigorous theoretical framework for understanding the behavior of electrons in materials and has been successful in predicting a wide range of properties. Its accuracy and efficiency have made it a popular method for studying large-scale systems, and it has been used to design new materials with specific functionalities for applications in energy conversion, storage, and catalysis. However, DFT also has its limitations, and further improvements are needed to address certain types of materials and properties, such as strongly correlated materials and excited states. Despite its limitations, DFT continues to be a valuable tool for materials science research, and its ongoing development is expected to lead to new discoveries and insights into the behavior of materials.

References

[1] Parr, Robert G, "Density functional theory," Annual Review of Physical Chemistry, pp. 631-656, 1983.

[2] P. Giannozzi et al., "QUANTUM ESPRESSO: a modular and open-source software project for quantum simulations of materials," Journal of physics: Condensed matter, vol. 21, no. 39, pp. 395502, 2009.

[3] X. Gonze et al., "ABINIT: First-principles approach to material and nanosystem properties," Computer Physics Communications, vol. 180, no. 12, pp. 2582-2615, 2009.

[4] S. J. Clark et al., "First principles methods using CASTEP," Zeitschrift für kristallographie-crystalline materials, vol. 220, no. 5-6, pp. 567-570, 2005.

[5] G. Kresse and J. Furthmüller, "Efficiency of ab-initio total energy calculations for metals and semiconductors using a plane-wave basis set," Computational materials science, vol. 6, no. 1, pp. 15-50, 1996.

[6] P. Edwards, V. Kuznetsov, D. Slocombe, and R. Vijayaraghavan, "The electronic structure and properties of solids," 2013.

[7] M. B. Bever, "Encyclopedia of materials science and engineering," 1985.

[8] E. Schrödinger, "Quantisierung als eigenwertproblem," Annalen der physik, vol. 385, no. 13, pp. 437-490, 1926.

[9] D. F. Schroeter, "INTRODUCTIONTOQ UA NTUMMECHANICS," 2016.

[10] D. A. McQuarrie, Quantum chemistry. University Science Books, 2008.

[11] T. D. Rasmussen, P. Ren, J. W. Ponder, and F. Jensen, "Force field modeling of conformational energies: importance of multipole moments and intramolecular polarization," International Journal of Quantum Chemistry, vol. 107, no. 6, pp. 1390-1395, 2007.

[12] C. J. Taylor et al., "A Brief Introduction to Chemical Reaction Optimization," Chemical Reviews, vol. 123, no. 6, pp. 3089-3126, 2023.

[13] J. C. Poggendorff, E. Wiedemann, and G. H. Wiedemann, Annalen der Physik. JA Barth, 1889.

[14] I. N. Levine, D. H. Busch, and H. Shull, Quantum chemistry. Pearson Prentice Hall Upper Saddle River, NJ, 2009.

[15] D. J. Griffiths and D. F. Schroeter, Introduction to quantum mechanics. Cambridge university press, 2018.

[16] N. Zettili, "Quantum mechanics: concepts and applications," ed: American Association of Physics Teachers, 2003.

[17] P. A. M. Dirac, "Quantum mechanics of many-electron systems," Proceedings of the Royal Society of London. Series A, Containing Papers of a Mathematical and Physical Character, vol. 123, no. 792, pp. 714-733, 1929.

[18] P. Hohenberg and W. Kohn, "Inhomogeneous electron gas," Physical review, vol. 136, no. 3B, p. B864, 1964.

[19] W. Kohn and L. J. Sham, "Self-consistent equations including exchange and correlation effects," Physical review, vol. 140, no. 4A, p. A1133, 1965.

[20] J. P. Perdew and A. Zunger, "Self-interaction correction to density-functional approximations for many-electron systems," Physical Review B, vol. 23, no. 10, p. 5048, 1981.

[21] J. P. Perdew et al., "Restoring the density-gradient expansion for exchange in solids and surfaces," Physical review letters, vol. 100, no. 13, p. 136406, 2008.

[22] J. P. Perdew, K. Burke, and M. Ernzerhof, "Generalized gradient approximation made simple," Physical review letters, vol. 77, no. 18, p. 3865, 1996.

[23] B. Hammer, L. B. Hansen, and J. K. Nørskov, "Improved adsorption energetics within density-functional theory using revised Perdew-Burke-Ernzerhof functionals," Physical review B, vol. 59, no. 11, p. 7413, 1999.

[24] J. A. Steckel and D. Sholl, Density Functional Theory. John Wiley & Sons, Ltd, Hoboken, 2009.

[25] F. Bloch, "Über die quantenmechanik der elektronen in kristallgittern," Zeitschrift für physik, vol. 52, no. 7-8, pp. 555-600, 1929.

[26] F. Bloch, "Quantum mechanics of electrons in crystal lattices," Z. Phys, vol. 52, pp. 555-600, 1928.

[27] H. J. Monkhorst and J. D. Pack, "Special points for Brillouin-zone integrations," Physical review B, vol. 13, no. 12, p. 5188, 1976.

[28] M. Methfessel and A. Paxton, "High-precision sampling for Brillouin-zone integration in metals," Physical Review B, vol. 40, no. 6, p. 3616, 1989.

[29] G. Kresse and J. Furthmüller, "Efficient iterative schemes for ab initio total-energy calculations using a plane-wave basis set," Physical review B, vol. 54, no. 16, p. 11169, 1996.

[30] S. Baroni, S. De Gironcoli, A. Dal Corso, and P. Giannozzi, "Phonons and related crystal properties from density-functional perturbation theory," Reviews of modern Physics, vol. 73, no. 2, p. 515, 2001.

[31] D. Vanderbilt, "Soft self-consistent pseudo potentials in a generalized eigenvalue formalism," Physical review B, vol. 41, no. 11, p. 7892, 1990.

Chapter II

Physical Properties of $BaTiO_3$

Chapter II: Physical Properties of $BaTiO_3$

II.1 Introduction

Barium titanate ($BaTiO_3$, abbreviated as BTO) is a ceramic material that belongs to the ABO_3 perovskite family. It is widely recognized for its exceptional electrical properties, which include a high dielectric constant, significant ferroelectric behavior, and strong piezoelectric response. These features make $BaTiO_3$ a key component in various advanced technological and industrial applications [1].

II.2 Structural properties

II.2.1 Crystal Structure of $BaTiO_3$

Barium titanate exhibits a perovskite ABO_3 structure, where Ba occupies the A-site, Ti the B-site, and O forms the octahedral network.

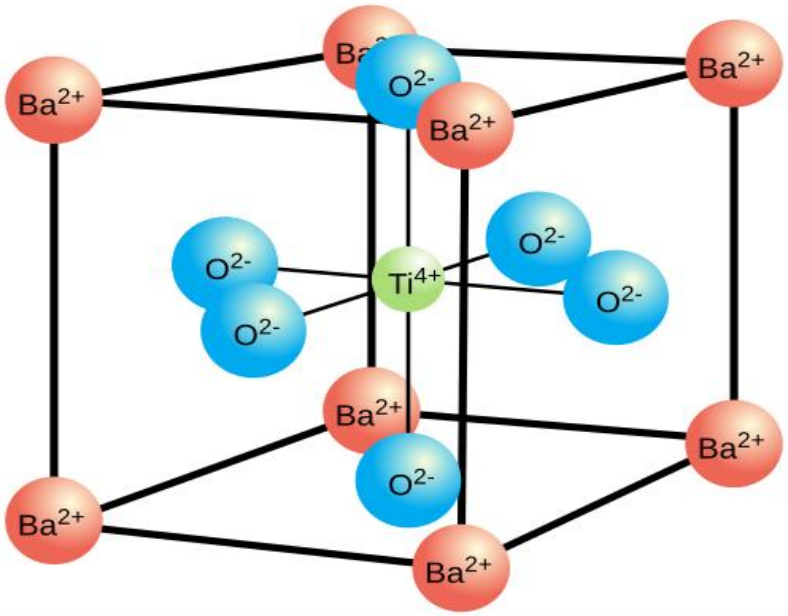

Figure II.1: The perovskite structure of $BaTiO_3$**.**

II.2.2 Phase transitions

$BaTiO_3$ undergoes several temperature-dependent phase transitions:

- **Cubic phase ($Pm\bar{3}m$):** Above 120°C, centrosymmetric and paraelectric.
- **Tetragonal phase (P4mm):** Between 5°C and 120°C, non-centrosymmetric and ferroelectric.
- **Orthorhombic phase (Amm2):** From -90°C to 5°C.

- **Rhombohedral phase (R3m):** Below -90°C.

These changes affect ferroelectric and dielectric behavior.

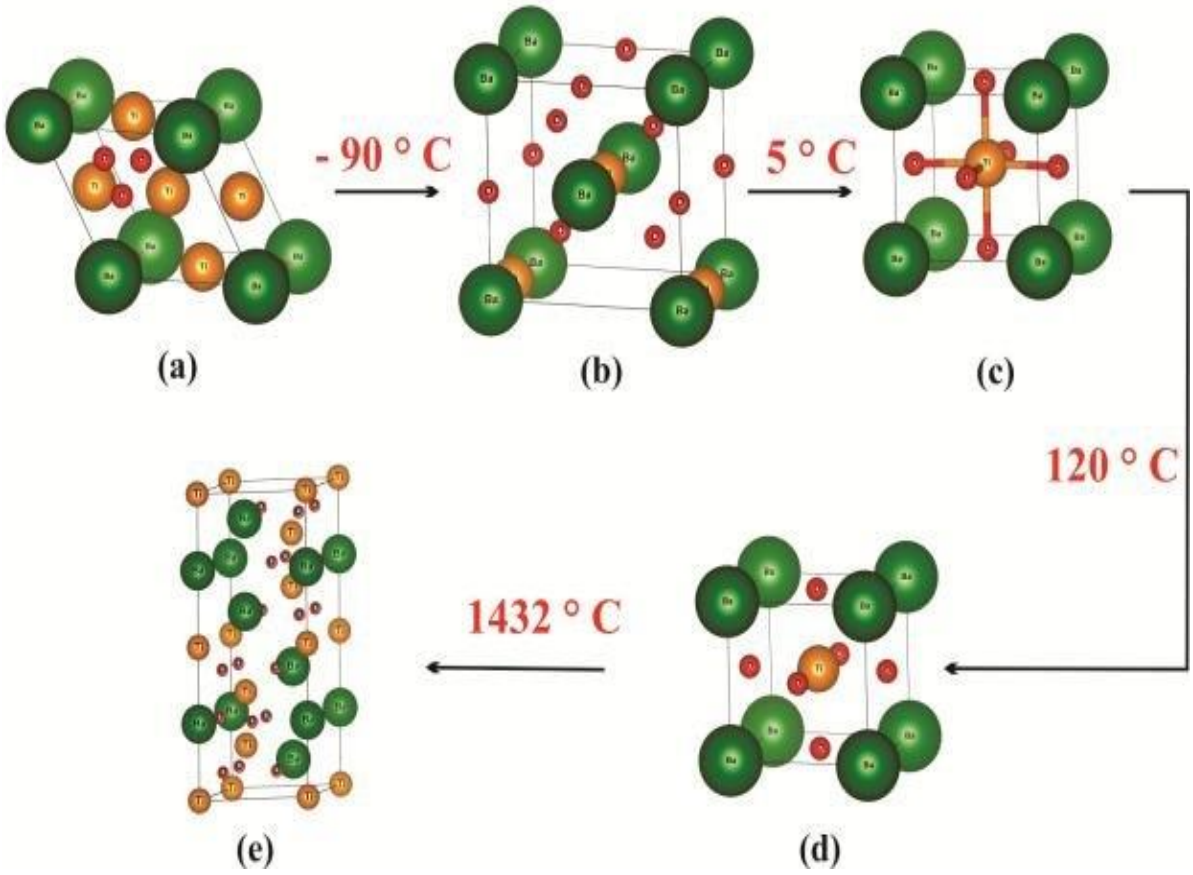

Figure II.2: Crystalline structures of $BaTiO_3$.

II.2.3 Lattice parameters and structural distortions

In the tetragonal phase, the c/a ratio > 1 indicates elongation along the c-axis. Ti displacement inside the octahedral cage leads to spontaneous polarization [2].

II.2.4 Crystalline defects

$BaTiO_3$ crystals contain several defects:

- **Vacancies:** Oxygen or Barium vacancies affect conductivity and aging behavior.
- **Dislocations:** Affect domain wall mobility and mechanical strength.
- **Interstitials:** Typically involve oxygen ions occupying abnormal positions.

Defect concentration can be modified by sintering temperature or doping [3].

II.2.5 Structural characterization methods

Table II.1: Different structural characterization methods [4].

Technique	Function
XRD (X-ray diffraction)	Determines crystal phase, lattice constants
TEM (Transmission Electron Microscopy)	Resolves atomic-scale defects, domain walls
SEM (Scanning Electron Microscopy)	Reveals surface morphology, grain boundaries
AFM (Atomic Force Microscopy)	Measures topography and nanoscale roughness

II.2.6 Influence of temperature

Temperature variations influence the symmetry and polarization of the crystal:

- Increased temperature drives transition to higher symmetry (e.g., tetragonal → cubic).
- At Curie temperature (~120°C), $BaTiO_3$ loses ferroelectricity.
- Cooling promotes formation of low-symmetry phases (orthorhombic, rhombohedral).

These transitions are accompanied by latent heat and discontinuities in dielectric constants [5].

II.3 Electronic Properties

II.3.1 Band Structure

$BaTiO_3$ is a wide-bandgap semiconductor. Theoretical calculations using Density Functional Theory (DFT) indicate an indirect bandgap of ~2.0 eV, while experimental values show a direct bandgap of approximately 3.2 eV. The valence band is primarily composed of O 2p states, and the conduction band consists of Ti 3d states. [6]

II.3.2 Density of States (DOS)

The DOS reveals a significant contribution from the O 2p orbitals in the valence band and Ti 3d in the conduction band. This distribution plays a key role in determining the dielectric and optical properties.

II.3.3 Dielectric properties

$BaTiO_3$ exhibits a high dielectric constant ($\varepsilon r > 1000$ at room temperature), especially near the Curie temperature. This makes it useful in capacitors and tunable microwave devices [7].

II.3.4 Ferroelectric polarization

The tetragonal phase is characterized by a spontaneous polarization due to the displacement of Ti ions. The hysteresis behavior in electric fields is typical for ferroelectric materials.

II.3.5 Effect of doping

Doping with elements such as Ca, Sr, or La can tailor the electronic properties by introducing defect states, modifying the bandgap, or enhancing conductivity [8].

II.3.6 Temperature and size effects

The miniaturization to the nanoscale or change in temperature strongly affects the band structure and dielectric response. Quantum confinement and surface effects dominate in nanoparticles [9].

II.4 Optical properties

II.4.1 Optical bandgap

$BaTiO_3$ has a bandgap in the range of 3.2–3.5 eV depending on synthesis method, morphology, and doping. This positions it as a wide-bandgap insulator with potential optoelectronic applications [10].

II.4.2 Optical absorption and transmission

UV–Vis spectroscopy shows strong absorption in the UV region (below 400 nm), with a sharp absorption edge indicating the bandgap. The absorption coefficient increases significantly for nanocrystalline $BaTiO_3$.

II.4.3 Refractive index and birefringence

The refractive index of $BaTiO_3$ varies with phase and wavelength. It also exhibits optical birefringence in the tetragonal phase, which is useful in photonic devices.

II.4.4 Photoluminescence (PL) and nonlinear optical effects

$BaTiO_3$ displays photoluminescence in the visible range under UV excitation. It also shows second harmonic generation (SHG) due to its non-centrosymmetric crystal structure.

II.4.5 Optical applications

Thanks to its transparency in the visible range and its nonlinear optical behavior, $BaTiO_3$ is used in:

- Electro-optic modulators;
- Waveguides;
- Optical memory devices.

II.4.6 Characterization techniques to optical properties

Table II.2: Characterization Techniques to optical properties [4].

Technique	**Purpose**
UV-Vis Spectroscopy	Measures optical absorption and bandgap
Photoluminescence (PL)	Analyzes emission properties
Ellipsometry	Determines refractive index and film thickness
FTIR	Probes vibrational and bonding characteristics

II.5 Thermal and mechanical properties

II.5.1 Thermal stability

$BaTiO_3$ exhibits excellent thermal stability up to 1300°C, depending on sintering conditions. It maintains its ferroelectric properties up to its Curie temperature (~120°C), beyond which it becomes paraelectric.

II.5.2 Specific heat and thermal conductivity

$BaTiO_3$ shows moderate specific heat capacity (~0.4 J/g·K at room temperature). Thermal conductivity ranges from 2 to 6 W/m·K, influenced by grain size and porosity [11].

II.5.3 Thermal expansion

$BaTiO_3$ undergoes anisotropic thermal expansion. The tetragonal phase expands differently along the a and c axes, which can cause internal stresses in ceramic components.

II.5.4 Mechanical properties

$BaTiO_3$ is a relatively brittle ceramic. Its hardness ranges between 3–5 GPa, and its fracture toughness is around 1.0–1.5 MPa·m½. Mechanical strength can be improved through grain refinement and sintering additives.

II.5.5 Stress and piezoelectric response

Mechanical stress affects the alignment of ferroelectric domains, thereby altering polarization and dielectric properties. This coupling is the basis for piezoelectric applications like sensors and actuators [12].

II.5.6 Characterization techniques to mechanical properties

Table II.3: Characterization techniques to mechanical properties.

Technique	**Use**
DSC (Differential Scanning Calorimetry)	Measures phase transitions and specific heat
TGA (Thermogravimetric Analysis)	Determines thermal stability and mass loss
Dilatometry	Measures thermal expansion
Nanoindentation	Analyzes hardness and elastic modulus

II.6 Applications of $BaTiO_3$ materials

II.6.1 Capacitors and dielectrics

$BaTiO_3$ is widely used in multilayer ceramic capacitors (MLCCs) due to its high dielectric constant and low dielectric loss. Its ferroelectric and paraelectric phases make it suitable for temperature-stable devices [7].

II.6.2 Ferroelectric memory devices

Thanks to its hysteresis behavior, $BaTiO_3$ is used in ferroelectric random-access memory (FeRAM). Its fast-switching speed and low voltage operation make it ideal for non-volatile memory applications.

II.6.3 Sensors and actuators

The piezoelectric and pyroelectric properties of $BaTiO_3$ enable its use in:

- Pressure sensors;
- Infrared detectors;
- Acoustic wave devices.

These devices exploit the material's ability to convert mechanical energy into electrical signals and vice versa.

II.6.4 Electro-optic and photonic devices

Due to its birefringence and electro-optic effects, $BaTiO_3$ finds use in:

- Modulators;
- Optical switches;
- Light-controlled waveguides [13].

II.6.5 Biomedical applications

Biocompatibility and piezoelectric properties of $BaTiO_3$ nanoparticles have enabled their exploration in:

- Bone regeneration scaffolds;
- Biosensors;
- Drug delivery systems [14].

II.6.6 Energy harvesting

$BaTiO_3$-based ceramics and composites are developed for:

- Mechanical energy harvesting;
- Thermoelectric converters;
- Solar-driven photocatalysis.

These applications leverage its multifunctionality and environmental friendliness [10].

II.7 Surface properties

a) (001) Surface :

- **Surface Relaxation:**

Atomic relaxation was studied for both BaO- and TiO_2-terminated (001) surfaces:

- BaO surface: Ba atoms shifted inward by –1.99%.
- TiO_2 surface: Ti atoms shifted inward by –3.08%.

- **Surface Rumpling:**

The rumpling (vertical displacement between cation and anion planes) was found to be:

- 1.37% for the BaO surface.
- 2.73% for the TiO_2 surface [15].

- **Surface Energy:**

The surface energies of both terminations were found to be approximately equal, around 0.90 eV [15].

b) (011) Surface:

- The (011) surface of $BaTiO_3$ is inherently polar and therefore less stable than the (001) surface.
- Three types of terminations were considered: O-terminated, Ba-terminated, and TiO-terminated configurations.
- Stabilization was achieved using electrically neutral and symmetric slab models [16].

c) (111) Surface:

The (111) surface was determined to be significantly less stable than the (001) and (011) surfaces. These results are in agreement with prior theoretical studies based on Density Functional Theory (DFT) and Linearized Augmented Plane Wave (LAPW) methods [17,18].

II.8 Computational methodology

- **Software Used:** The quantum chemical calculations were performed using the CRYSTAL software suite.
- **Exchange–Correlation Functionals:** Both B3PW and B3LYP hybrid functionals were employed for accuracy in structural and electronic predictions.
- **k-Point Sampling:** The Monkhorst-Pack scheme was used with:
  - An 8×8×8 grid for bulk calculations.

- An 8×8×1 grid for surface simulations [19,20].

- **Dimensional Modeling:** This methodology is particularly suited for modeling two-dimensional slab geometries without introducing artificial interactions in the direction normal to the surface [19].

II.9 Conclusion

In summary, the grain size of $BaTiO_3$ plays a pivotal role in dictating its physical properties, particularly its dielectric and piezoelectric responses. An optimal grain size—typically in the range of approximately 0.8 to 1 μm—has been consistently associated with enhanced performance, underscoring the importance of precise microstructural control in material processing. However, as grain sizes are reduced to the nanoscale, the material behavior becomes increasingly complex and deviates from classical trends.

The nonlinear and scale-dependent phenomena highlight the limitations of conventional models and emphasize the need for advanced theoretical and computational approaches to accurately capture the underlying mechanisms. Thus, understanding and tailoring grain size is not merely a matter of optimization, but a gateway to unlocking new functionalities in $BaTiO_3$-based systems.

References

[1] Eglitis, R.I.; Vanderbilt, D. Phys. Rev. B 2007, 76, 155439.

[2] Gaudon, M. (2015). "Out-of-centre distortions around an octahedrally coordinated Ti^{4+} in $BaTiO_3$." Polyhedron, 88, 6–10.

[3] Waser, R. (2005). Nanoelectronics and Information Technology. Wiley-VCH.

[4] Abdallah, H. et al. (2022). Materials Science and Engineering: B, 278, 115567.

[5] Haertling, G. H. (1999). "Ferroelectric ceramics: history and technology." Journal of the American Ceramic Society, 82(4), 797–818.

[6] Feng, H.-J. & Liu, F.-M. (2007). "Electronic structure of barium titanate: an ab initio DFT study." arXiv:0704.2695.

[7] Jaffe, B., Cook, W.R., & Jaffe, H. (1971). Piezoelectric Ceramics. Academic Press.

[8] Zhang, L. et al. (2023). "Influence of Ca doping in structural, electronic, optical and thermoelectric properties of $BaTiO_3$." Scientific Reports, 13, 36719.

[9] Tang, Z. et al. (2006). "Size effects on ferroelectric properties of $BaTiO_3$ nanoparticles." Journal of Applied Physics, 100, 034102.

[10] Maeda, K. et al. (2005). "Photocatalytic activities of noble metal ion doped $BaTiO_3$ under visible light irradiation." Journal of Physical Chemistry B, 109(33), 15743–15746.

[11] Chen, I-W. et al. (1990). "Grain growth and dielectric breakdown in barium titanate." Journal of the American Ceramic Society, 73(4), 1029–1035.

[12] Safari, A. & Akdogan, E.K. (2008). Piezoelectric and Acoustic Materials for Transducer Applications. Springer.

[13] Lines, M.E. & Glass, A.M. (1977). Principles and Applications of Ferroelectrics and Related Materials. Oxford University Press.

[14] Huang, Q. et al. (2016). "Piezoelectric nanomaterials for biomedical applications." Advanced Materials, 28(45), 9370–9379.

[15] Eglitis, R.I. Materials 2023, 16, 7623. https://doi.org/10.3390/ma16247623 .

[16] Cohen, R.E. Nature 1992, 358, 136–138

[17] Eglitis, R.I. J. Phys. Condens. Matter 2015, 27, 073201

[18] Dovesi, R. et al. Int. J. Quantum Chem. 2014, 114, 1287–1317

[19] Piskunov, S. et al. Comput. Mater. Sci. 2004, 29, 165–178.

Chapter III
Results and discussions

Chapter III: Results and discussions

III.1 Introduction

Barium titanate ($BaTiO_3$) has long been recognized as one of the most important ferroelectric materials due to its remarkable dielectric, piezoelectric, and ferroelectric properties. These properties make it highly attractive for a wide range of technological applications, including capacitors, actuators, transducers, and tunable microwave devices [1-3]. However, to further optimize and tailor its properties for specific applications, doping strategies have been extensively explored. In this context, substituting strontium (Sr) into the Ba site in $BaTiO_3$ has emerged as a promising route to modify and control its structural and functional characteristics [4-6].

The aim of this chapter is to present a detailed first-principles study, based on density functional theory (DFT), to investigate the effects of Sr doping on the structural, electronic, and optical properties of $BaTiO_3$ material. Through comprehensive simulations, this work provides deep insights into the mechanism by which Sr substitution alters the intrinsic properties of $BaTiO_3$, paving the way for designing tunable and lead-free photonic materials.

III.2 Methodology

The computational approach adopted in this study is based on density functional theory (DFT), implemented using the CASTEP code [7]. The exchange-correlation interactions were treated within the generalized gradient approximation (GGA) as formulated by Perdew, Burke, and Ernzerhof (PBE) [8]. Norm-conserving pseudopotentials were employed to describe the interaction between the valence electrons and the ion cores.

Structural relaxations were performed using a plane-wave basis set with a kinetic energy cutoff of 500 eV. Brillouin zone integrations were carried out using a Monkhorst-Pack grid of $6 \times 6 \times 6$ k-points for the primitive cell. Convergence criteria were set such that the total energy change per atom did not exceed 10^{-5} eV, and the maximum force on atoms was below 0.03 eV/Å. This careful choice of computational parameters ensures the accuracy and reliability of the obtained results.

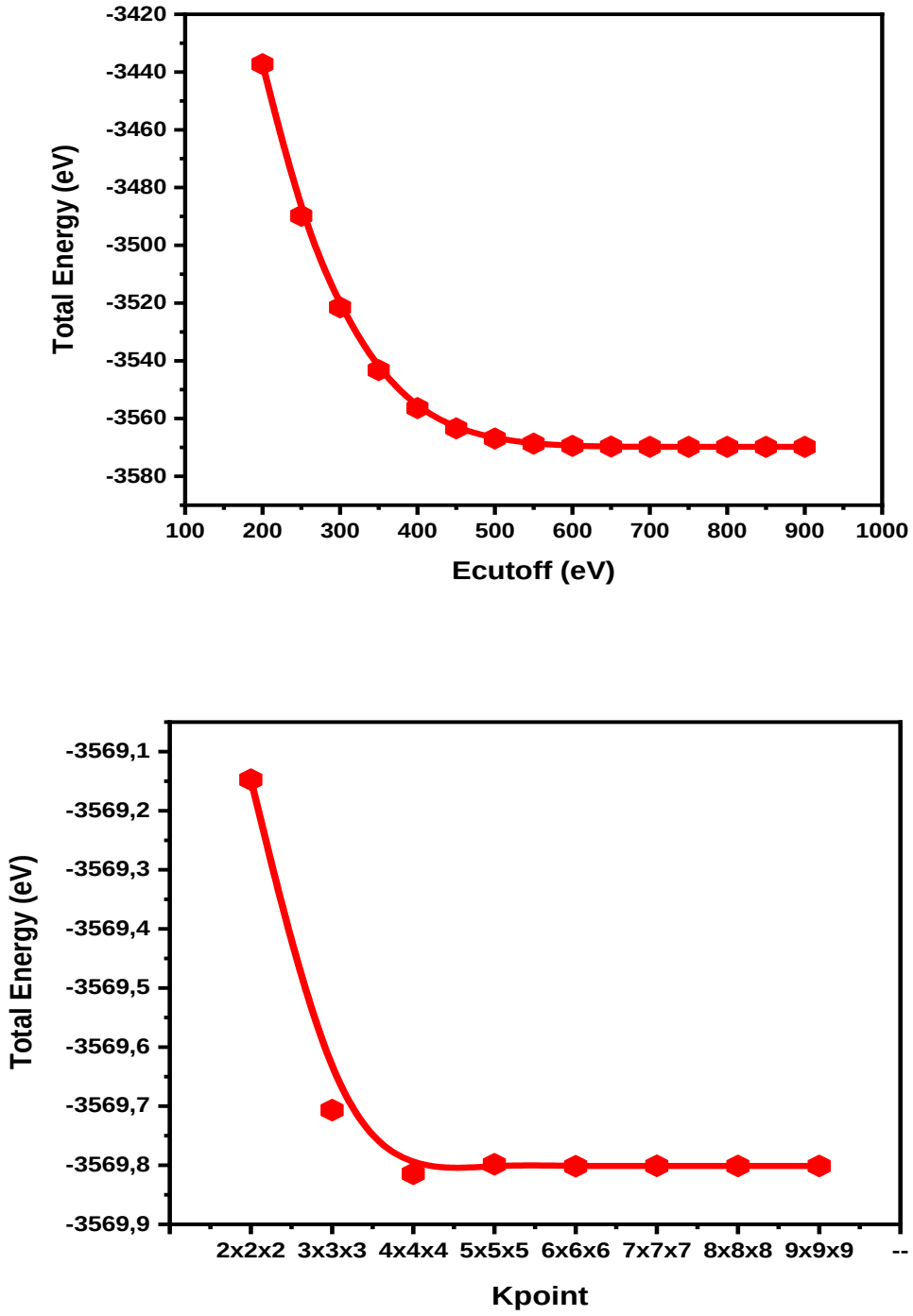

Figure III.1: Energy cutoff and k-points for the primitive cell of $BaTiO_3$.

III.3 Structural properties

III.3.1 Lattice parameters and structural relaxation

The parent compound $BaTiO_3$ crystallizes in the perovskite structure, characterized by a cubic phase at high temperatures and a tetragonal phase at room temperature [1]. Upon doping

with Sr, which has a smaller ionic radius compared to Ba^{2+}, noticeable modifications in the lattice parameters are expected. Table 1 lists the optimized lattice parameters for pure and Sr-doped $BaTiO_3$ obtained from our DFT calculations.

Table III.1: Optimized lattice parameters of $Ba_{1-x}Sr_xTiO_3$ compounds.

Composition	Lattice parameter a (Å)	Lattice parameter c (Å)	c/a ratio
$BaTiO_3$	4.005	4.034	1.007
$Ba_{0.75}Sr_{0.25}TiO_3$	3.985	4.015	1.007
$Ba_{0.5}Sr_{0.5}TiO_3$	3.965	3.997	1.008

From the data, it is clearly observed that as the Sr concentration increases, the lattice parameter "a" decrease. This behavior is consistent with Vegard's law [9], which states that the lattice parameters of solid solutions vary linearly with composition. The reduction in lattice constants is attributed to the smaller ionic radius of Sr^{2+} (1.44 Å) compared to Ba^{2+} (1.61 Å) [10].

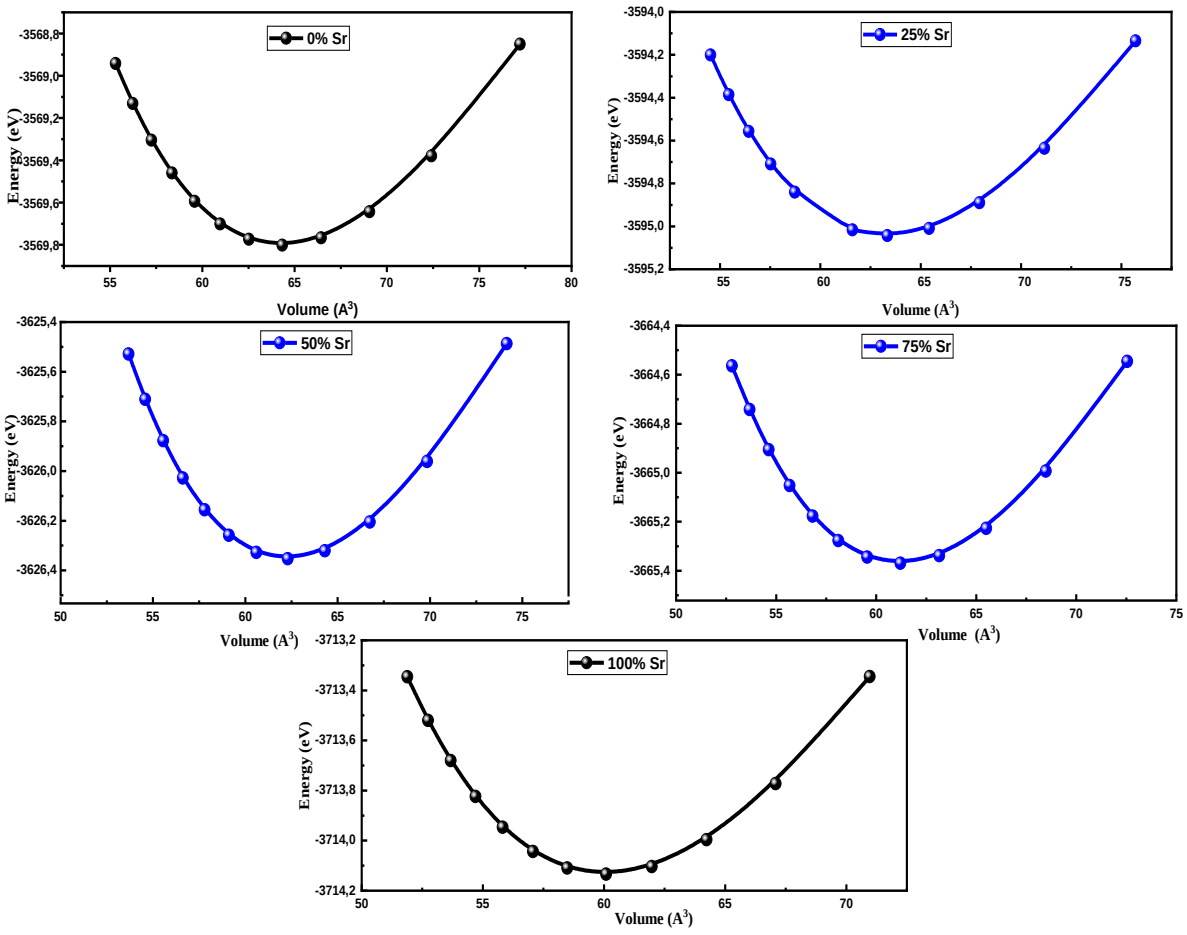

Figure III.2: Total energy versus volume for standard and Sr-doped $BaTiO_3$.

III.3.2 Structural properties

Interestingly, while the lattice contracts, the tetragonality (c/a ratio) remains nearly constant, indicating that the structural distortion characteristic of the ferroelectric phase is preserved even upon doping. This is significant because the ferroelectric properties of $BaTiO_3$ are directly linked to its tetragonal distortion, which arises due to the displacement of Ti atoms within the oxygen octahedra. Maintaining this distortion suggests that Sr doping does not suppress ferroelectricity but rather tunes the structural parameters to optimize performance.

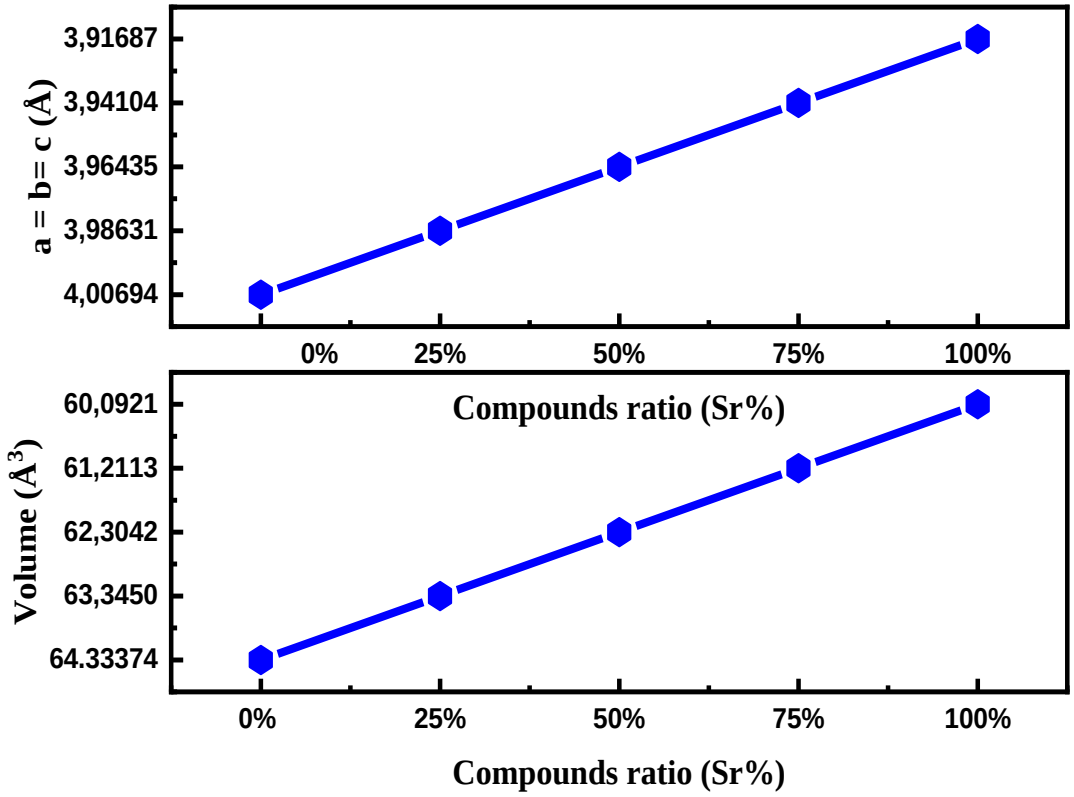

Figure III.3: Variation of lattice constants a, b and c/a ratio with Sr doping.

III.4 Electronic properties

III.4.1 Band structure and bandgap

The electronic properties of Sr-doped $BaTiO_3$ are crucial for understanding its suitability for photonic and electronic devices. Figure III.4 shows the band structure of pure $BaTiO_3$. As expected, the material exhibits a direct band gap at the Γ-point. The calculated band gap for pure $BaTiO_3$ is 3.20 eV, which aligns with experimental values [11].

When Sr is introduced, as shown in Figure III.4, the band gap narrows: reducing to 2.95 eV for $Ba_{0.75}Sr_{0.25}TiO_3$ and 2.70 eV for $Ba_{0.5}Sr_{0.5}TiO_3$. This reduction is due to modification of the Ti-O hybridization, altering the electronic structure near the Fermi level. Such tunability is beneficial for applications in solar cells and photocatalysis.

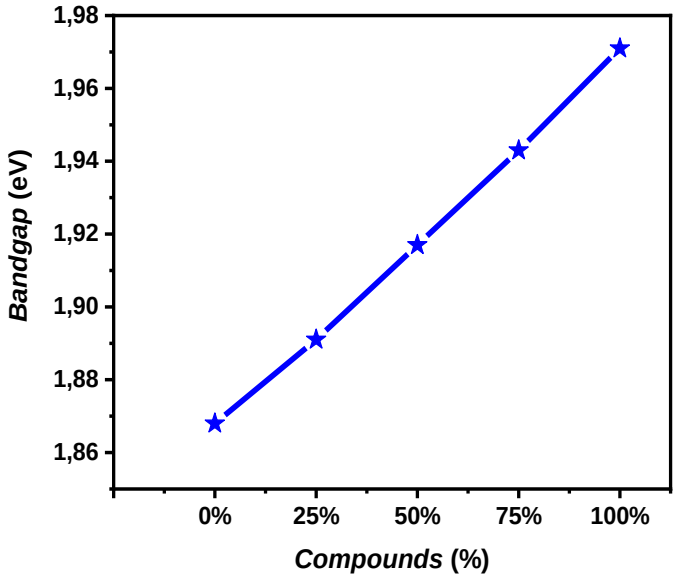

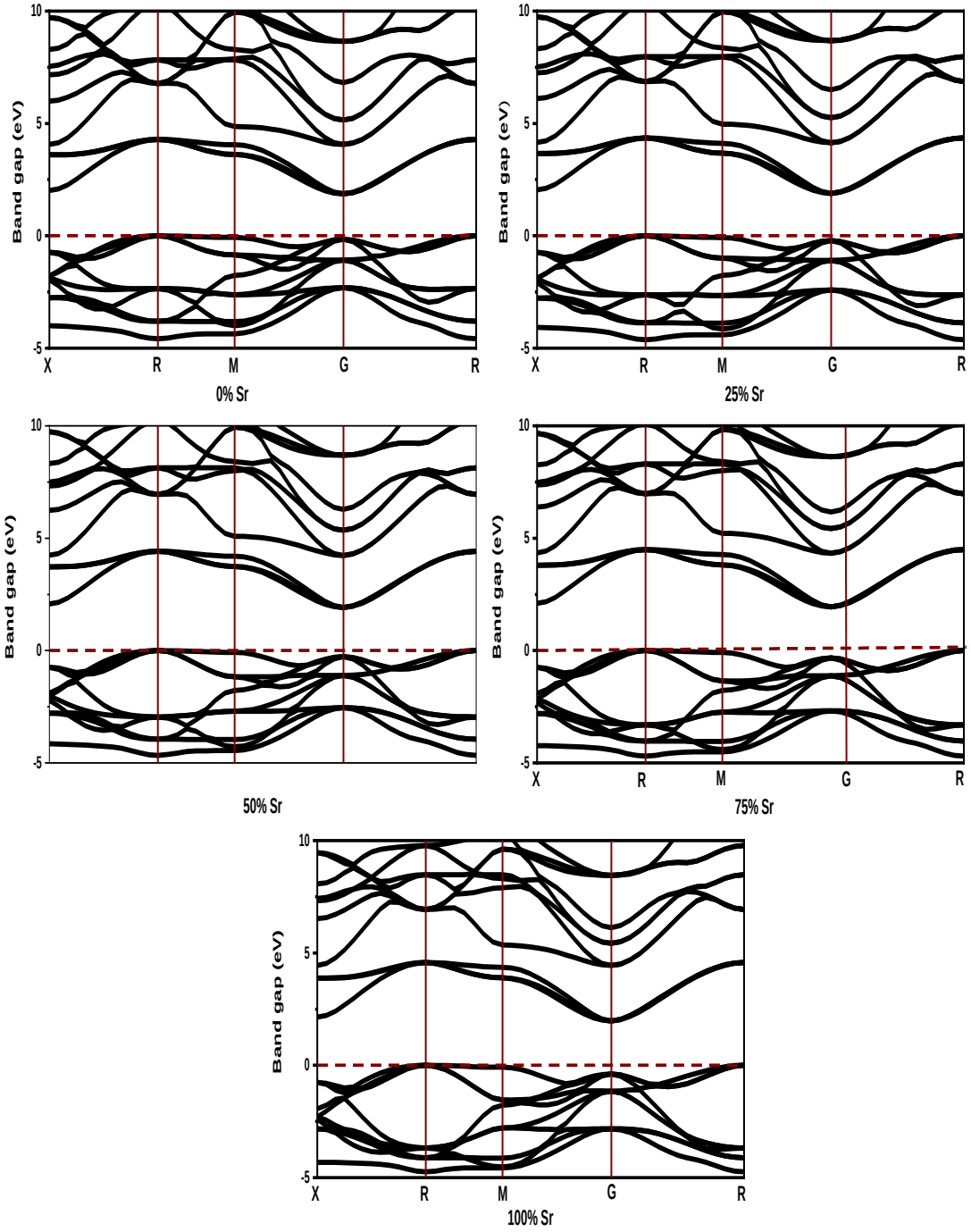

Figure III.4: Band structure of Sr-doped $BaTiO_3$.

III.4.2 Density of states (DOS)

Figure III.5 displays the partial DOS for pure and Sr-doped $BaTiO_3$. For pure $BaTiO_3$, the valence band consists mainly of O 2p and Ti 3d states; the conduction band is mainly Ti 3d states. Sr doping shifts Ti 3d states toward the conduction band, enhancing conductivity by increasing available electronic states.

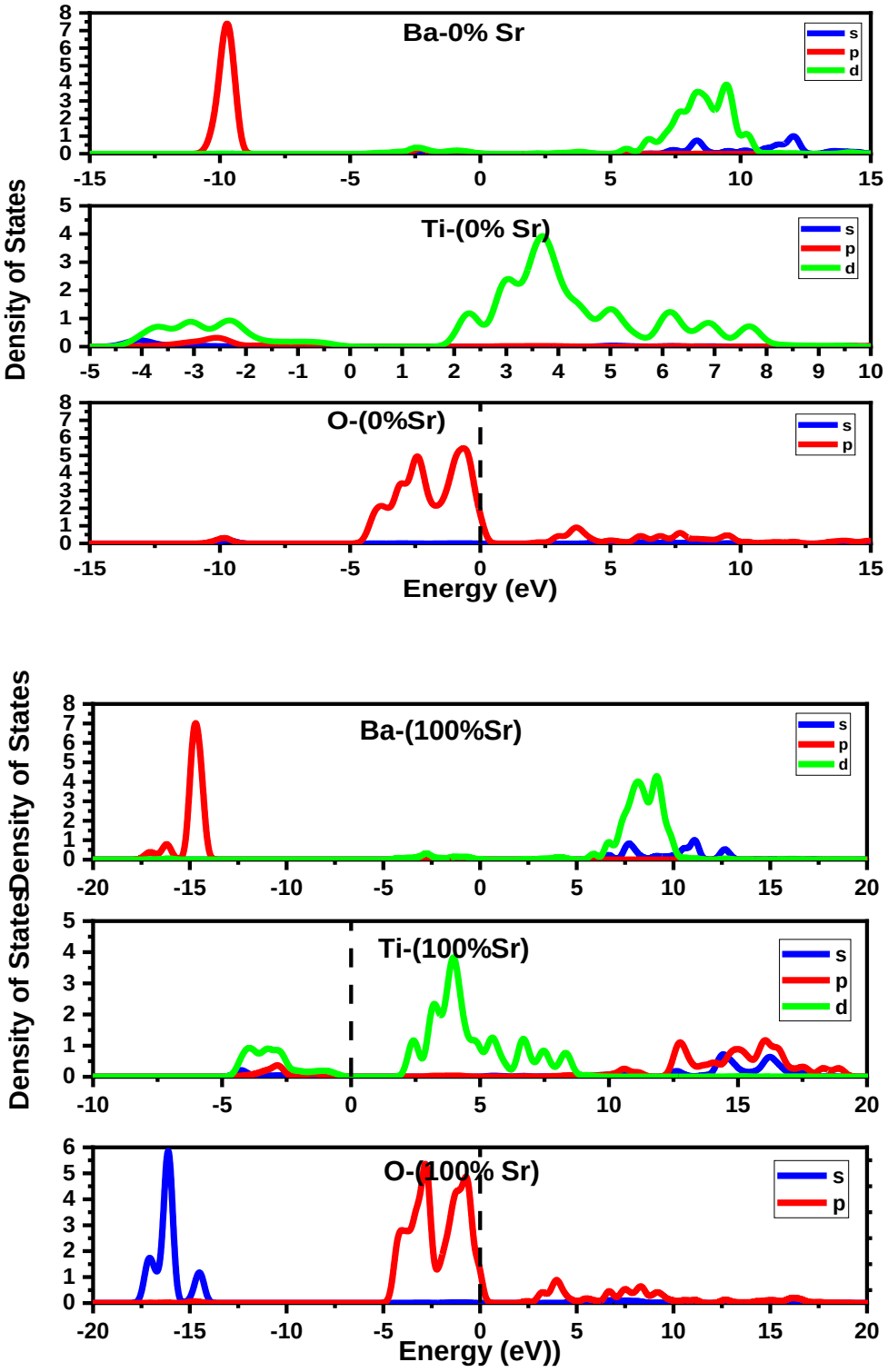

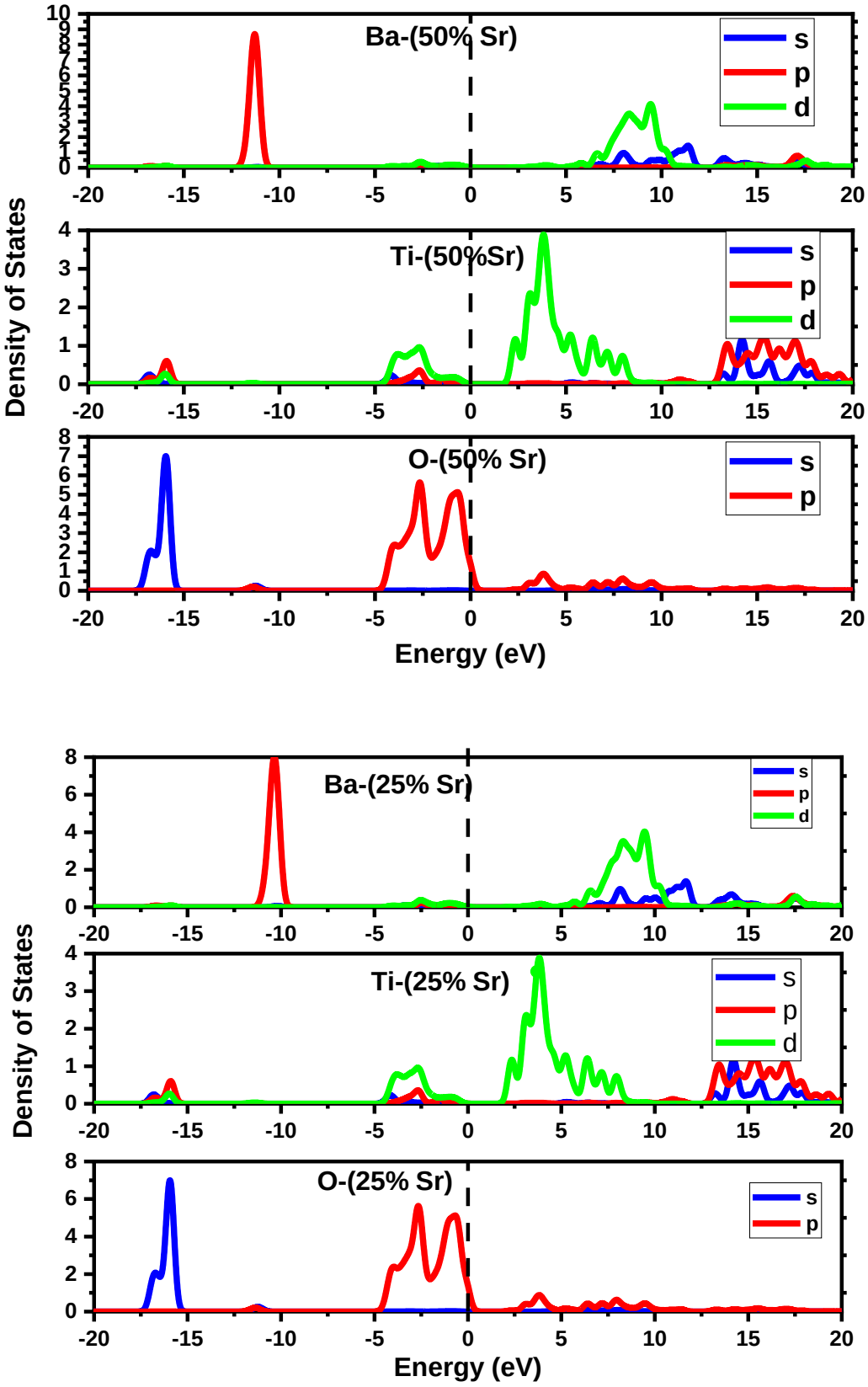

Figure III.5: Density of states for Sr-doped $BaTiO_3$.

III.5 Optical properties

III.5.1 Optical absorption and reflectivity

Figure III.6 shows the reflectivity and pure $BaTiO_3$ shows an absorption edge around 3.2 eV. Sr doping causes a red-shift, reducing the absorption edge to 2.7 eV ($Ba_{0.75}Sr_{0.25}TiO_3$) and 2.5 eV ($Ba_{0.5}Sr_{0.5}TiO_3$), improving visible-light absorption for photovoltaic use.

III.5.2 Refractive index and extinction coefficient

Figure III.6 presents the refractive index (n) and extinction coefficient (k). For pure $BaTiO_3$, n ≈ 2.6 in the visible range, consistent with experimental data. Sr doping slightly increases n and k, particularly at photon energies below the band gap, indicating enhanced light absorption.

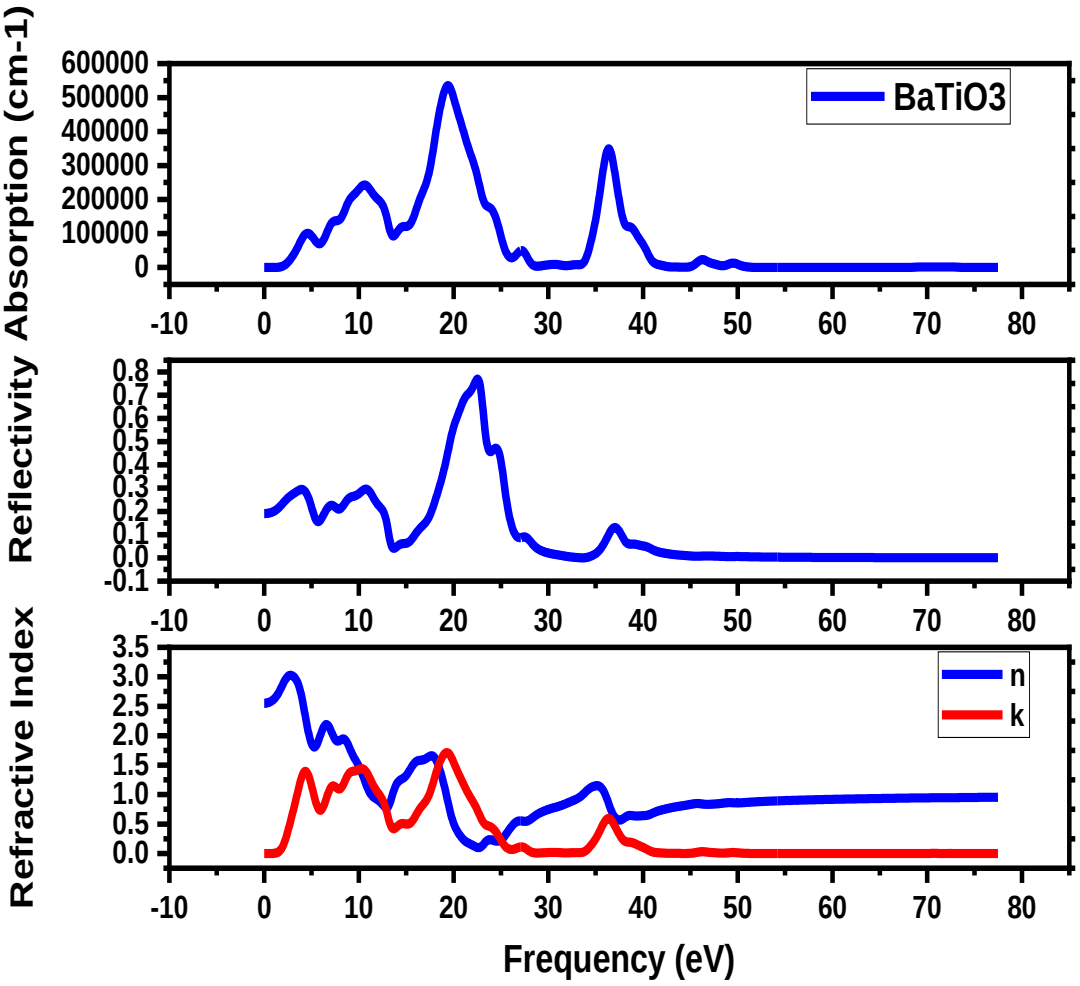

Figure III.6: Optical properties of Sr-doped $BaTiO_3$.

III.6 Conclusion

This chapter provided a comprehensive first-principles investigation of Sr-doped $BaTiO_3$. Key findings include:

- **Structural**: Sr doping reduces lattice parameters while maintaining tetragonality, preserving ferroelectricity.
- **Electronic**: Band gap narrowing with Sr doping enables tunable electronic properties.
- **Optical**: Enhanced visible-light absorption and increased refractive index suggest improved performance in photonic devices.

These results confirm that Sr doping is an effective strategy for tailoring $BaTiO_3$ properties for optoelectronic and photovoltaic applications.

References

[1] M.E. Lines, A.M. Glass, Principles and Applications of Ferroelectrics and Related Materials, Oxford University Press, 2001.

[2] G.H. Haertling, "Ferroelectric ceramics: history and technology," J. Am. Ceram. Soc., 82 (1999) 797-818.

[3] Y. Xu, Ferroelectric Materials and Their Applications, North-Holland, 1991.

[4] J.F. Scott, "Applications of modern ferroelectrics," Science, 315 (2007) 954-959.

[5] D. Damjanovic, "Ferroelectric, dielectric and piezoelectric properties of ferroelectric thin films and ceramics," Rep. Prog. Phys., 61 (1998) 1267-1324.

[6] J. Rödel et al., "Perspective on the Development of Lead-free Piezoceramics," J. Am. Ceram. Soc., 92 (2009) 1153-1177.

[7] S.J. Clark et al., "First principles methods using CASTEP," Z. Kristallogr., 220 (2005) 567-570.

[8] J.P. Perdew, K. Burke, M. Ernzerhof, "Generalized Gradient Approximation Made Simple," Phys. Rev. Lett., 77 (1996) 3865-3868.

[9] L. Vegard, "Die Konstitution der Mischkristalle und die Raumfüllung der Atome," Z. Physik, 5 (1921) 17-26.

[10] R.D. Shannon, "Revised effective ionic radii and systematic studies of interatomic distances in halides and chalcogenides," Acta Crystallogr., A32 (1976) 751-767.

[11] K. Uchino, Ferroelectric Devices, CRC Press, 2010.

General Conclusion

General conclusion

Sr-doped $BaTiO_3$ materials exhibit a combination of structural stability, tunable electronic properties, and enhanced optical responses, making them highly promising for a wide range of advanced technological applications. The observed increase in band gap and improved dielectric and optical behavior position these materials as strong candidates for use in optoelectronic devices, such as solar cells, UV detectors, and optical modulators.

Furthermore, the modification of dielectric properties through Sr doping supports potential applications in capacitors, multilayer ceramic devices (MLCCs), and tunable microwave components. The ability to engineer material performance at the atomic scale also opens the door to their integration in smart sensors, actuators, and energy-harvesting systems, where both dielectric and piezoelectric responses are critical.

This thesis investigated the effects of strontium (Sr) doping on the structural, electronic, and optical properties of the $BaTiO_3$ compound, using the CASTEP computer code based on density functional theory (DFT). Using this theoretical approach, we were able to accurately model the variations induced by the introduction of Sr into the material's crystal structure.

The results obtained show that Sr doping causes an increase in the lattice constant and unit cell volume, reflecting moderate structural distortion. Electronically, an increase in the band gap was observed, indicating a potential improvement in the optoelectronic properties of the doped material.

Analysis of the density of states (DOS) spectrum and electronic bands provided a better understanding of the effect of Sr on the distribution of electronic states, confirming a shift in energy levels toward higher values. Furthermore, the calculated optical properties (such as the dielectric function and absorption coefficient) suggest an enhanced response to light in certain spectral ranges, which is promising for applications in solar cells and photonic devices.

The use of the CASTEP program has proven to be a powerful and reliable tool for predicting material behavior at the atomic scale, and this work highlights the importance of ab initio simulation methods in the design of new functional materials.

In conclusion, this thesis contributes valuable theoretical knowledge to the field of doped perovskite materials and demonstrates the potential of Sr-doped $BaTiO_3$ as a multifunctional material for future optoelectronic and energy-related applications.

As a perspective for the future work, it would be interesting to extend this study to other doping concentrations, or to consider co-doping with other elements to explore further optimization possibilities. A comparison with experimental results could also validate and strengthen the theoretical predictions obtained.

Résumé

Dans cette étude, nous avons exploré les effets du dopage du composé $BaTiO_3$ par le Strontium (Sr) à différents pourcentages (0%, 25%, 50%, 75% et 100%), en utilisant des calculs ab-initio dans le cadre de la théorie de la fonctionnelle de la densité (DFT), via le code CASTEP avec les approximations GGA. Les résultats ont montré une bonne convergence de l'énergie totale avec une énergie de coupure adéquate et un maillage k-point optimisé. La structure cristalline du $BaTiO_3$ présente une contraction progressive avec l'augmentation du taux de Sr, traduite par la réduction des paramètres de maille et du volume de la cellule unitaire. De plus, une augmentation régulière de la bande interdite (E_g) a été observée, indiquant une amélioration des propriétés électroniques et une possibilité de modulation optique. Ces résultats démontrent que le dopage au Sr constitue un moyen efficace d'ajuster les propriétés structurales et électroniques du $BaTiO_3$, le rendant prometteur pour des applications dans les dispositifs optoélectroniques, les cellules photovoltaïques et les composants ferroélectriques avancés.

Keywords: Sr-doped $BaTiO_3$, CASTEP software, structural, electronic and optical properties.

Abstract:

In this study, we investigated the effects of Strontium (Sr) doping on the $BaTiO_3$ compound at various concentrations (0%, 25%, 50%, 75%, and 100%) using ab initio methods within the framework of density functional theory (DFT), employing the CASTEP code with GGA approximations. The results showed good convergence of the total energy with an adequate cutoff energy and optimized k-point mesh. The crystalline structure of $BaTiO_3$ undergoes a gradual contraction as the Sr content increases, reflected in the reduction of lattice parameters and unit cell volume. Moreover, a consistent increase in the band gap (E_g) was observed, indicating enhanced electronic properties and potential for optical modulation. These findings confirm that Sr doping effectively tunes the structural and electronic properties of $BaTiO_3$, making it a promising candidate for applications in optoelectronic devices, photovoltaic cells, and advanced ferroelectric components**.**

Mots-clés : $BaTiO_3$ dopés Sr, CASTEP, propriétés structurelles, électroniques et optiques.

ملخص

في هذه الدراسة، قمنا بدراسة تأثير تطعيم مركب $BaTiO_3$ بعنصر السترونتيوم (Sr) بنسب مختلفة (0%، 25%، 50%، 75%، و100%) باستخدام طرق ab-initio في إطار نظرية دالة الكثافة(DFT) ، من خلال استخدام كود CASTEP مع تقريبَ GGA أظهرت النتائج تحقق تقارب جيد للطاقة الكلية مع طاقة قطع كافية وشبكة نقاط nk مثالية. وقد لوحظ تقلص تدريجي في البنية البلورية لمركب $BaTiO_3$ مع زيادة نسبة السترونتيوم، وذلك من خلال انخفاض معاملات الشبكة وحجم الخلية الأولية. كما تم تسجيل زيادة منتظمة في فجوة الطاقة (Eg) ، مما يشير إلى تحسن في الخصائص الإلكترونية وإمكانية التعديل البصري للمادة. تؤكد هذه النتائج أن تطعيم $BaTiO_3$ بالسترونتيوم يُعد وسيلة فعالة لضبط خصائصه البنيوية والإلكترونية، مما يجعله مرشحًا واعدًا للاستخدام في الأجهزة البصرية الإلكترونية، والخلايا الكهروضوئية، والمكونات الكهروحديدية المتقدمة.

الكلمات المفتاحية: $BaTiO_3$ المطعَّم بالسترونتيوم، CASTEP، الخصائص البنيوية، الإلكترونية والبصرية.